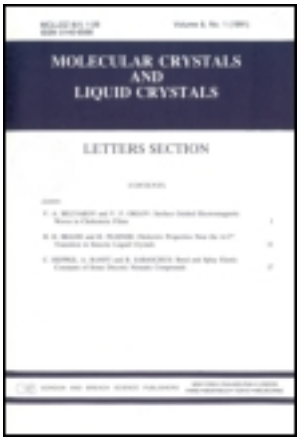

Molecular Crystals and Liquid Crystals
Publication details, including instructions for authors and subscription information:
http://www.tandfonline.com/loi/gmcl20

Enhanced Performance of Organic Photovoltaic Cells by Incorporation of a Cyanobiphenyl Compound into Active Layer

Yoon Soo Han [a]

[a] Department of Advanced Energy Material Science and Engineering , Catholic University of Daegu , Gyeongbuk , 712-702 , Korea

Published online: 08 Jan 2014.

To cite this article: Yoon Soo Han (2013) Enhanced Performance of Organic Photovoltaic Cells by Incorporation of a Cyanobiphenyl Compound into Active Layer, Molecular Crystals and Liquid Crystals, 586:1, 43-52, DOI: 10.1080/15421406.2013.851458

To link to this article: http://dx.doi.org/10.1080/15421406.2013.851458

Mol. Cryst. Liq. Cryst., Vol. 586: pp. 43–52, 2013

ISSN: 1542-1406 print/1563-5287 online
DOI: 10.1080/15421406.2013.851458

Taylor & Francis
Taylor & Francis Group

Enhanced Performance of Organic Photovoltaic Cells by Incorporation of a Cyanobiphenyl Compound into Active Layer

YOON SOO HAN*

Department of Advanced Energy Material Science and Engineering, Catholic University of Daegu, Gyeongbuk 712-702, Korea

*The effect of an additive, 4-cyano-4'-pentylbiphenyl (5CB), on the performance of organic photovoltaic cells (OPVs) has been demonstrated. The addition of 3wt% 5CB to a P3HT [poly(3-hexylthiophene)]:PCBM [[6,6]-phenyl-C61-butyric acid methyl ester] blend film resulted in an improvement of both fill factor (*FF*) and short circuit current (J_{sc}), and hence increased the overall power conversion efficiency by over 22% compared to that of reference cell without 5CB. Carrier mobility studies and optical measurements revealed that the increase in* FF *in the OPV with 5CB was attributed to more balanced ratio of hole and electron mobility, resulting from the enhanced crystallization of the P3HT chains, which can increase hole mobility. This ordering of P3HT also led to an increase in* J_{sc}.

Keywords Additive; organic photovoltaic cell; P3HT; PCBM; power conversion efficiency

Introduction

In the last decade, interest in solid-state organic photovoltaic cells (OPVs) has grown remarkably due to their low manufacturing costs, light weight, and flexibility as well as their potential for large-scale production through roll-to-roll processing such as flexographic printing, slot die coating, and rotary screen printing [1–6]. Since the vapor-deposited donor/acceptor bilayer devices [7] with a low power conversion efficiencies (PCEs) of 1% was reported by Tang in 1986 and the first bulk heterojunction (BHJ) OPV [1] based on conjugated polymer-fullerene blends showed a PCE of 2.9% in 1995, there have been steady improvements in PCEs of OPVs. However, their low *PCE*s are still a major obstacle to their commercial utilization. The main limiting factors for the PCE of OPVs are poor exciton/charge transport and narrow absorption in the visible range of the solar spectrum in the active layer. The donor and acceptor materials should form nano-scaled interpenetrating networks within the whole active layer to ensure efficient exciton dissociation and charge transport [8]. Therefore, significant studies for improving light harvesting, photocurrent generation and exciton/charge transport in the active layer have had a morphological basis. Several interesting methods, including thermal annealing [9,10], solvent annealing [11],

*Address correspondence to Y. S. Han, Department of Advanced Energy Material Science and Engineering, Catholic University of Daegu, 13-13 Hayang-ro, Hayang-eup, Gyeongsan-si, Gyeongbuk 712-702, Korea. Tel.: +82-53-850-2773, Fax: +82-53-850-3292. E-mail: yshancu@cu.ac.kr

microwave annealing [12], and processing additives [13] or non-volatile additives into the active layer [14] have been used to effectively control the morphology and subsequently improve the performance of OPVs.

In particular, the incorporation of additives into a blend film composed of electron donor and acceptor materials is regarded to be the best method for improving the morphology and photovoltaic performance of the OPVs due to its ease of applicability [13,15]. Various processing additives [13,15–22] have been used in OPVs with [6,6]-phenyl-C61-butyric acid methyl ester (PCBM; electron acceptor) and poly(3-hexylthiophene) (P3HT; electron donor).

In this study, a compound with nematic liquid crystal phase near room temperature, 4-cyano-4'-pentylbiphenyl (5CB), was used as an additive in P3HT:PCBM-based OPVs to improve device efficiency. OPVs with a configuration of ITO/PEDOT:PSS/P3HT:PCBM with or without 5CB/LiF/Al were fabricated, and their photovoltaic properties were investigated.

Experimental Details

Materials

P3HT (98% regioregularity, $M_w = 6.4 \times 10^4$ g/mol) and $PC_{61}BM$ were purchased from Rieke Metals and Nano-C, respectively. Poly-3,4-ethyleneoxythiophene:poly-4-sytrensulfonate (PEDOT:PSS, Baytron P VP Al 4083) was used as received from P. H. Stark GmbH. Solvents used in this study were all reagent grade and were used as received unless stated otherwise. 5CB was purchased from Tokyo Chemical Industry Co., Ltd., and used without further purification. The chemical structure of the 5CB additive in this study is shown in Fig. 1.

Device Fabrication

OPVs were fabricated on indium-tin oxide (ITO) glasses (10 Ω/□, SUNIC Ltd.) as follows. ITO glasses were cleaned by sequential ultrasonication in acetone, detergent, de-ionized water and isopropyl alcohol and then dried in a vacuum oven. Next, O_2 plasma treatment of the ITO glasses was conducted for 3 min, and immediately afterwards, PEDOT:PSS was spin-coated onto the ITO glass. The PEDOT:PSS films were then baked on a hot plate for 15 min at 140 °C to yield a thickness of 30 nm; the film-coated ITO glass was then moved to a N_2 glove box for the remainder of the fabrication process. Regioregular P3HT and PCBM at a weight ratio of 1:0.9 were first dissolved in chlorobenzene. Selected amounts of the 5CB additive, ranging from 2 to 5 wt% based on the P3HT:PCBM, were then added to the P3HT:PCBM solution, followed by stirring for 24 h at 50 °C. The solution consisting of P3HT:PCBM blended with or without additives was spin-cast onto the top of the PEDOT:PSS layer, and the plate was then dried on a hot plate in a covered Petri dish for 40 min at 50 °C to produce an active layer with a thickness of 120 nm. Finally, a cathode

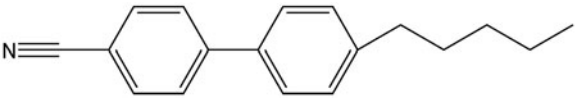

Figure 1. The chemical structure of 5CB.

consisting of LiF (1 nm) and a subsequent Al (100 nm) layer was deposited by thermal evaporation under a vacuum of 10^{-7} Torr. Devices with the configuration of ITO/PEDOT:PSS (30 nm)/P3HT:PCBM:with or without additive (120 nm)/LiF (1 nm)/Al (100 nm) were encapsulated with a glass cap to protect them from air and then thermally annealed for 25 min at 145 °C. The active area of all devices was determined to be 9 mm^2 using a shadow mask. Hole-only devices were fabricated with a diode configuration of ITO/PEDOT:PSS (30 nm)/P3HT:PCBM:with or without additive (120 nm)/Pd (100 nm), where Pd with a high work function was used as an electrode to prevent the injection of electrons to LUMO (lowest unoccupied molecular orbital) energy level of PCBM. By replacing PEDOT:PSS with a Cs_2CO_3 layer spin-coated from its solution in 2-ethoxyethanol, electron-only devices were fabricated with a diode configuration of ITO/Cs_2CO_3/P3HT:PCBM:with or without additive (120 nm)/LiF (1 nm)/Al (100 nm) for measuring electron mobility.

Characterization

UV-visible absorption spectra of the fabricated blend films with and without additive were obtained using a Perkin Elmer Lambda 750 UV/VIS spectrometer. The X-ray diffraction (XRD) profiles were measured using a BRUKER D8 ADVANCE with Cu Kα as the incident beam. Data were obtained from 3 ° to 50 ° (2θ) at a scan rate of 0.2 s/step. Photocurrent-voltage measurements were performed with a Keithley model 2400 Source Meter and a Newport 91192 solar simulator system equipped with 1-kW xenon arc lamp from Oriel. The light intensity was adjusted to simulate AM 1.5 radiation at 100 mW cm^{-2} with a Radiant Power Energy Meter (model 70260, Oriel). All measurements were carried out under ambient conditions at room temperature.

Results and Discussion

The devices with the configuration of ITO/PEDOT:PSS (30 nm)/P3HT:PCBM:with or without 5CB (120 nm)/LiF (1 nm)/Al (100 nm) were fabricated and characterized after thermal annealing treatment for 25 min at 145 °C. The amount of 5CB in the blend solution was varied from 0 to 5 wt% to optimize the performance of OPV devices. The photovoltaic properties of the devices characterized under AM 1.5 conditions as a function of 5CB amount are presented in Fig. 2. The PCEs of annealed devices with 2–4 wt% 5CB were considerably enhanced as compared to the control device (OPV0) without any additive, and fill factor (*FF*) and short circuit current (J_{sc}) values showed sensitivity to variation in the 5CB amount in the blend films. The annealed device (OPV3) with 3 wt% 5CB exhibited the best performance due to an enhancement in *FF* and J_{sc}, resulting in a PCE of 4.36% as compared to that (3.56%) of the control device (OPV0). Because the PCE exhibited the highest value when the 5CB content was 3 wt%, we focused on this device with P3HT:PCBM:5CB (3 wt%) blend film to determine the origin of the enhancement in efficiency. The photovoltaic properties of the annealed devices with and without 5CB are summarized in Table 1, and the current density (J) versus voltage (V) curves are illustrated in Fig. 3.

As described above, the improved performance of devices with 3 wt% 5CB resulted from an increase in both *FF* and J_{sc}. The enhanced *FF* of the annealed device with 3 wt% 5CB had a significant influence (68% contribution) on the PCE, as shown in Table I. It is generally accepted that the *FF* is influenced by the balance between hole and electron mobilities in OPVs because it is limited by the carrier drift length, which is defined as (carrier mobility) x (carrier recombination lifetime) x (electric field) [23,24]. Space charge

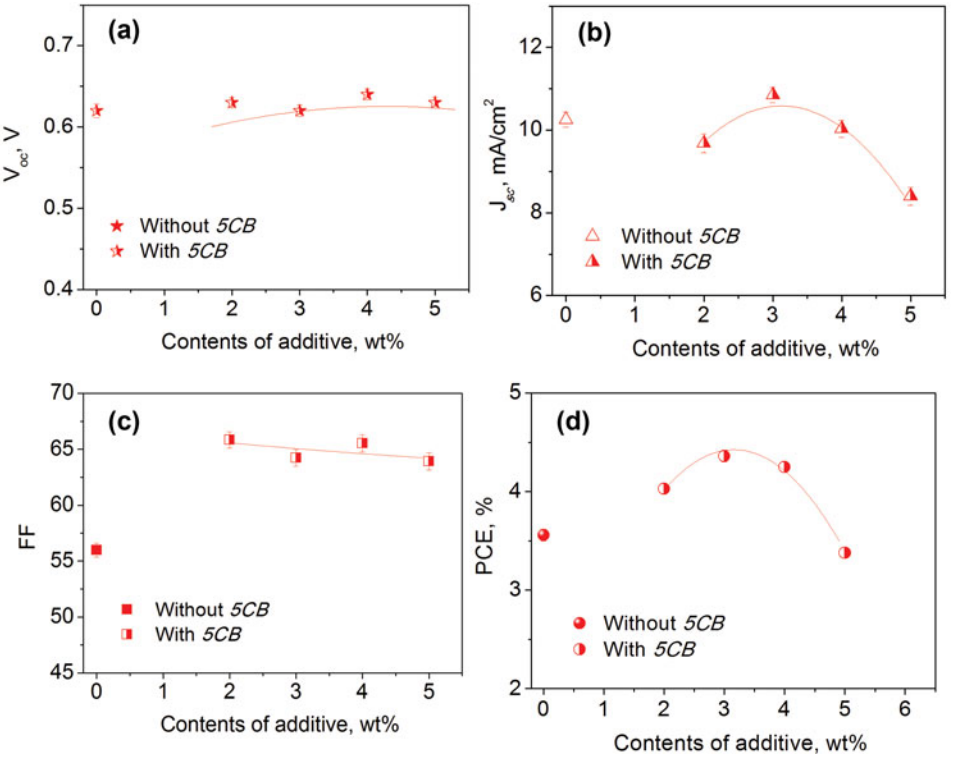

Figure 2. Performance variations with 5CB concentration; (a) V_{oc}, (b) J_{sc}, (c) *FF* and (d) *PCE* of annealed OPVs under AM 1.5 irradiation.

limited current (SCLC) measurements have been used to evaluate charge mobility under steady state currents in organic layers [25,26]. According to SCLC criteria, a half-power dependence of the photocurrent on the applied voltage is observed, and the *FF* cannot be above 40%. However, when the carrier transport is more balanced, the current is not limited by space-charge effects, and high *FF*s are possible [11].

Using the SCLC method, the hole mobility of the devices was studied to confirm the effect of the additive on the fill factor of the annealed devices. The current density in the SCLC model is given by equation (1).

$$J = \frac{9}{8}\varepsilon_r \varepsilon_0 \mu_{h0} \frac{V^2}{L^3} \exp\left(0.89\sqrt{\frac{V}{E_0 L}}\right) \tag{1}$$

Table 1. Photovoltaic properties of OPVs with and without 5CB

Annealed devices	Content of additive	V_{oc}, V	J_{sc}, mA/cm^2	*FF*,%	*PCE*,%
OPV0	0 wt%	0.62	10.25	55.98	3.56
OPV3	3 wt%	0.62	10.95	64.23	4.36

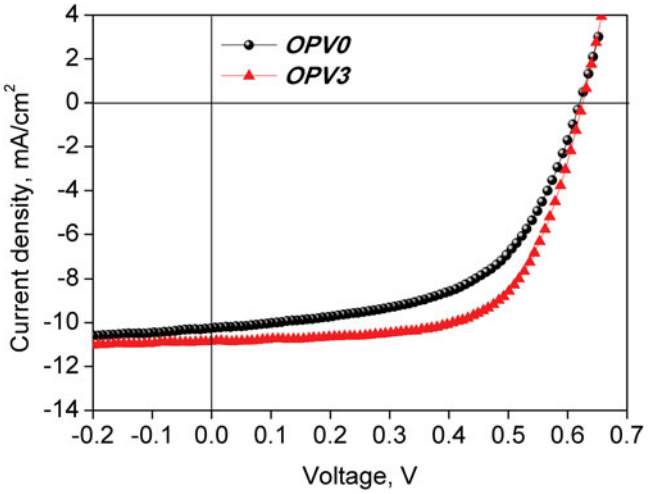

Figure 3. *J-V* characteristics of annealed OPVs with and without 5CB.

Here, ε_r is the dielectric constant of the polymer (assumed to be 3, which is a typical value for conjugated polymers) [27,28], ε_0 is the permittivity of free space, μ_{h0} (or μ_{e0}) is the zero-field hole (or electron) mobility, L is the film thickness, and E_0 is the characteristic field. $V = V_{appl} - (V_r + V_{bi})$, where V_{appl} is the voltage applied to the device, V_r is the voltage drop due to series resistance across the electrodes and V_{bi} is the built-in voltage. The hole mobilities of the devices were calculated from equation (1) using the *J-V* curves of the hole-only devices [25] with the configuration of ITO/PEDOT:PSS(30 nm)/P3HT:PCBM:with or without 5CB (120 nm)/Pd(100 nm), which can obstruct the electron injection from the cathode due to the large mismatch between the LUMO energy level (4.30 eV) of PCBM [29] and the work function (5.12 eV) of the Pd electrode [30], as illustrated in Fig. 4(a). The experimental dark current densities of the annealed hole-only devices with or without 5CB are shown in Fig. 5(a). The results are also plotted as the logarithm of JL^3/V^2 versus the square root of V/L, as shown in the inset of Fig. 5(a). In the inset graph, the intercept of this line represents the hole mobility. The hole mobility of the device with 3 wt% 5CB increased from 2.8×10^{-5} to 3.1×10^{-4} cm^2/V·s, one order of magnitude higher than that of the device without 5CB.

Meanwhile, electron-only devices with the configurations ITO/Cs_2CO_3/P3HT:PCBM: with or without 5CB/LiF/Al, in which Cs_2CO_3 layer [26] transports electrons from LUMO energy level of PCBM to ITO and blocks holes from ITO to HOMO (highest occupied molecular orbital) energy level of P3HT [Fig. 4(b)] were fabricated, and then the electron mobilities of the electron-only devices were calculated using equation (1) and measured

Table 2. Crystalline and mobility characteristics of P3HT in the annealed devices

Annealed devices	Additive content	P3HT crystallite (nm)	Hole mobility (cm^2/V·s)	Electron mobility (cm^2/V·s)	μ_e/μ_h
OPV0	0 wt%	16.0	2.8×10^{-5}	5.0×10^{-3}	178
OPV3	3 wt%	21.1	3.1×10^{-4}	7.5×10^{-3}	24

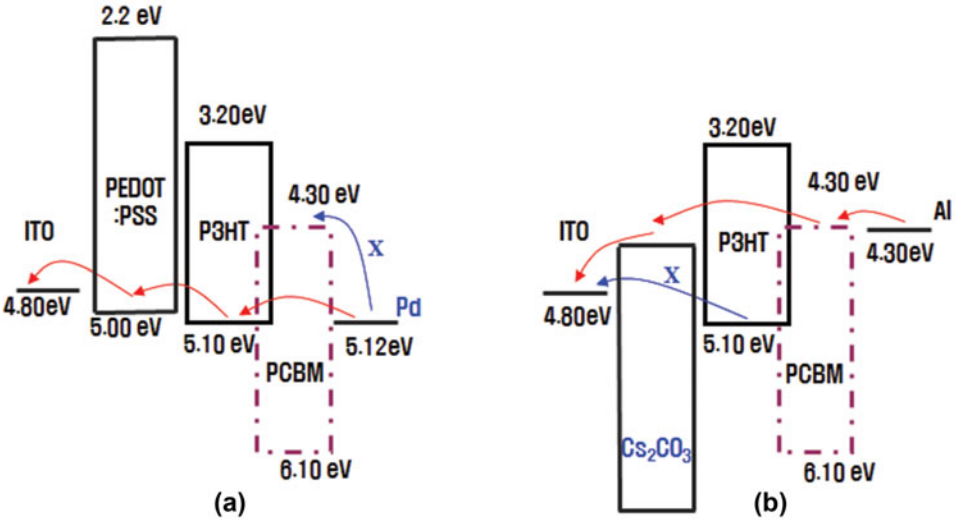

Figure 4. Energy band diagram of the hole-only and electron-only devices.

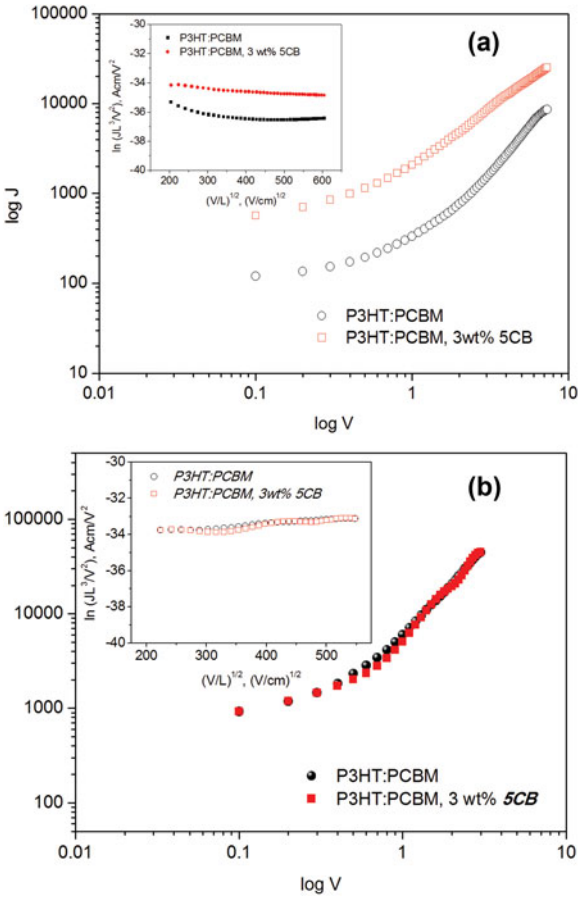

Figure 5. J-V characteristics of the hole-only (a) and electron-only (b) devices measured in the dark.

J-V data [Fig. 5(b)]. The electron mobility changed very little from 5.0×10^{-3} for the control device to 7.5×10^{-3} $cm^2/V{\cdot}s$ for the device with 5CB. Based on the calculated hole and electron mobilities, the ratio (μ_e/μ_h) of the hole and electron mobility for the devices with 5CB was determined to be 24 as compared to that (178) of the device without 5CB. Due to an enhanced and balanced charge transport in the device with the 5CB additive, a high *FF* of about 64.23% was achieved [31]. The photovoltaic performance of devices with a thicker active layer than the mean carrier drift length of the charge carrier is limited by the carrier with a lower mean free path (holes in OPVs) [32]. To maintain the electrical neutrality in the device, the unbalanced transport will result in loss of efficiency due to increased charge recombination. Significant enhancement of hole mobility by the addition of 5CB into the active layer yields more balanced transport of holes and electrons, and hence reduces the accumulation of space charges in films and hole-electron recombination loss, leading to an enhancement of the *FF* [33,34].

This enhancement in hole mobility could be attributed to more ordered P3HT chains in the presence of 5CB [35]. To reveal effects of 5CB on the ordering of P3HT in the P3HT:PCBM blend films, UV-visible absorption spectra of an annealed P3HT:PCBM:5CB blend film cast from a chlorobenzene solution on a quartz plate were compared with that of a pristine P3HT:PCBM film (Fig. 6). The annealed blend film with 3 wt% 5CB exhibited stronger absorption as compared to the pristine P3HT:PCBM blend film. Similar phenomena in P3HT:PCBM blend systems with various additives have been reported by several groups [36,37]. These studies revealed that the increased π-π^* transition band was attributed to enhanced crystallization of P3HT chains in devices with a small amount of additive.

The effect of 5CB on the ordered structure of P3HT was further investigated using X-ray diffraction (XRD) measurements. Figure 7 presents the XRD patterns of thermally annealed P3HT:PCBM films with and without 3 wt% 5CB on PEDOT:PSS/ITO glasses; these films exhibited strong P3HT reflections at major $d_{(100)}$ peaks [23,38,39]. The average crystal size (L) of the P3HT in P3HT:PCBM films was calculated from the full width at half maximum (FWHM) of the $d_{(100)}$ peaks in the P3HT crystals using Scherrer's equation [$L = K\lambda / (B\ cos\theta)$] [40], where λ is the incident X-ray wavelength, B is the FWHM of the diffraction $d_{(100)}$ peak, θ is the diffraction angle, and K is Scherrer's constant. The average

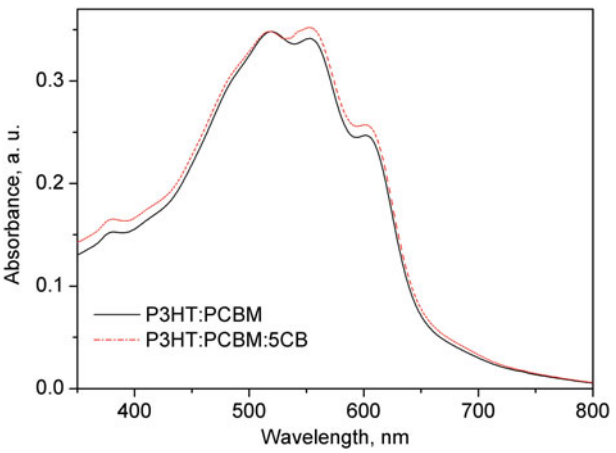

Figure 6. UV-vis absorption spectra of the P3HT:PCBM blend films with and without 5CB additive.

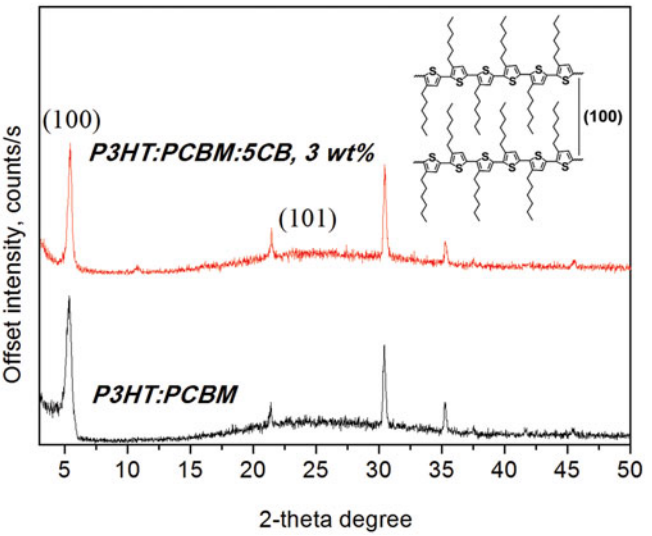

Figure 7. The X-ray diffractograms of annealed P3HT:PCBM blend films with and without 5CB. The peaks at $2\theta \approx 22^\circ$ and 31° arise from ITO [23,38], and the peak at $2\theta \approx 35^\circ$ is from PCBM [39].

crystal size of the P3HT in the P3HT:PCBM:5CB (3 wt%) blend film was calculated to be 21.1 nm, which is a slight increase of 5.1 nm as compared to that measured for the P3HT:PCBM film (16.0 nm). The improved ordering of P3HT due to the incorporation of 5CB additive in the blend film is expected to contribute to the enhancement in hole mobility.

As evidences of the enhanced hole mobility, above results such as stronger absorption and larger crystal size of P3HT chains could also have an direct influence on current level of the device with P3HT:PCBM: 5CB blend film. It is well known that the better interchain registry within ordered domains also plays an important role in increasing current density, i.e., J_{sc} of OPVs. Thus, we could conclude that J_{sc} enhancement of the device, corresponding to 32% contribution to improvement in PCE, was due to an increase in light harvesting and more effective charge transport properties by the ordering of P3HT [41,42].

The open circuit voltage (V_{oc}) maintained the same values of 0.62 V, as shown in Table 1. Because the V_{oc} is linearly related to the $HOMO_{donor}$-$LUMO_{acceptor}$ energy difference [43], which is directly correlated with acceptor strength, the same V_{oc} indicates that the acceptor strength in the OPVs was not changed by the addition of 5CB to the P3HT:PCBM-blend film.

Conclusion

In summary, we have investigated the effects of 5CB with nematic liquid crystal phase near room temperature on the photovoltaic properties of P3HT:PCBM-based OPVs. The devices fabricated using 5CB-incorporated P3HT:PCBM blend film achieved an PCE of 4.36% due to the improved *FF* and J_{sc}, compared to that (3.56%) of reference cell without 5CB additive. This result indicates that the introduction of 5CB induces efficient charge transport and collection, resulting from the enhanced P3HT crystallization and the correspondingly higher charge carrier mobility, as evidenced by the UV-vis absorption, XRD and charge mobility measurements.

Acknowledgments

This work was supported by research grants from the Catholic University of Daegu in 2012.

References

[1] Yu, G., Gao, J., Hummelen, J. C., Wudl, F., & Heeger, A. J. (1995). *Science*, *270*, 1789.
[2] Gunes, S., Neugebauer, H., & Sariciftci, N. S. (2007). *Chem. Rev.*, *107*, 1324.
[3] Helgesen, M., Søndergaard, R., & Krebs, F. C. (2010). *J. Mater. Chem.*, *20*, 36.
[4] Krebs, F. C., Tromholt, T., & Jøegense, M. (2010). *Nanoscale*, *2*, 873.
[5] Krebs, F. C., Fyenbo, J., & Jøegense, M. (2010). *J. Mater. Chem.*, *20*, 8994.
[6] Krebs, F. C., Gevorgyan, S. A. & Alstrup, J. (2010). *J. Mater. Chem.*, *19*, 5442.
[7] Tang, C. W. (1986). *Appl. Phys. Lett.*, *48*, 183.
[8] Sivula, K., Ball, T., Watanabe, N., & Fréchet, J. M. M. (2006). *Adv. Mater.*, *18*, 206.
[9] Nguyen, L. H., Hoppe, H., Erb, T., Günes, S., Gobsch, G., & Sariciftci, N. S. (2007). *Adv. Mater.*, *17*, 1071.
[10] Kim, K., Liu, J., Namboothiry, M. A. G., & Carroll, D. L. (2007). *Appl. Phys. Lett.*, *90*, 163511.
[11] Li, G., Shrotriya, V., Huang, J., Yao, Y., Moriarty, T., Emery, K., & Yang, Y. (2005). *Nat. Mater.*, *4*, 864.
[12] Ko, C.-J., Lin, Y.-K., & Chen, F.-C. (2007). *Adv. Mater.*, *19*, 3520.
[13] Peet, J., Kim, J. Y., Coates, N. E., Ma, W. L., Moses, D., Heeger, A. J., & Bazan, G. C. (2006). *Nat. Mater.*, *6*, 497.
[14] Kim, C. S., Tinker, L. L., DiSalle, B. F., Gomez, E. D., Lee, S., Bernhard, S., & Loo, Y.-L. (2009). *Adv. Mater.*, *21*, 3110.
[15] Chen, H.-Y., Hou, J. H., Zhang, S. Q., Liang, Y. Y., Yang, G. W., Yu, L. P., Wu, Y., & Li, G. (2009). *Nat. Photonics*, *3*, 649.
[16] Chang, Y.-M., & Wang, L. (2008). *J. Phys. Chem.*, *112*, 17716.
[17] Wu, I.-C., Lai, C.-H., Chen, D.-Y., Shih, C.-W., Wei, C.-Y., Ko, B.-T., Ting, C., & Chou, P.-T. (2008). *J. Mater. Chem.*, *18*, 4297.
[18] Honda, S., Nogami, T., Ohkita, H., Benten, H., & Ito, S. (2009). *ACS Appl. Mater. Interfaces*, *1*, 804.
[19] Ismail, Y. A. M., Soga, T., & Jimbo, T. (2009). *Sol. Energy Mater. Sol. Cells*, *93*, 1582.
[20] Jeong, S., Kwon, Y.-H., Choi, B.-D., Ade, H., & Han, Y. S. (2010). *Appl. Phys. Lett.*, *96*, 183305.
[21] Jeong, S., Kwon, Y., Choi, B.-D., Kwak, G., & Han, Y. S. (2010). *Macromol. Chem. Phys.*, *211*, 2474.
[22] Jeong, S., Woo, S.-H., Lyu, H.-K., & Han, Y. S. (2011). *Sol. Energy Mater. Sol. Cells*, *95*, 1908.
[23] Ma, W. L., Yang, C. Y., Gong, X., Lee, K., & Heeger, A. J. (2005). *Adv. Funct. Mater.*, *15*, 1617.
[24] Koster, L. J. A., Mihailetchi, V. D., & Blom, P. W. M. (2006). *Appl. Phys. Lett.*, *88*, 093511.
[25] Chirvase, D., Chiguvare, Z., Knipper, M., Paris, J., Dyakonov, V., & Hummelen, J. C. (2003). *J. Appl. Phys.*, *93*, 3376.
[26] Shrotriya, V., Yao, Y., Li, G., & Yang, Y. (2006). *Appl. Phys. Lett.*, *89*, 063505.
[27] Kim, S.-O., Chung, D. S., Cha, H., Jang, J. W., Kim, Y.-H., Kang, J.-W., Jeong, Y.-S., Park, C. E., & Kwon, S.-K. (2011). *Sol. Energy Mater. Sol. Cells*, *95*, 432.
[28] Zhou, H., Yang, L., Stoneking, S., & You, W. (2010). *ACS Appl Mater Interfaces*, *2*, 1377.
[29] Kim, J. Y., Lee, K., Coates, N. E., Moses, D., Nguyen, T.-Q., Dante, M., & Heeger, A. J. (2007). *Science*, *317*, 222.
[30] Gu, D., Deya, S. K., & Majhi, P. (2006). *Appl. Phys. Lett.*, *89*, 082907.
[31] Chiu, M., Jeng, U., Su, M., & Wei, K. (2010). *Macromolecules*, *43*, 428.
[32] Snaith, H. L., Greenham, N. C., & Friend, R. H. (2004). *Adv. Mater.*, *16*, 1640.
[33] Shin, C. F., Hung, K. T., Wu, J. W., Hsiao, C. Y., & Li, W. M. (2009). *Appl. Phys. Lett.*, *94*, 143505.
[34] Liu, J., Shao, S., Wang, H., Zhao, K., Xue, L., Gao, X., Xie, Z., & Han, Y. (2010). *Org. Electron.*, *11*, 775.

[35] Kim, Y., Cook, S., Tuladhar, S. M., Choulis, S. A., Nelson, J., Durrant, J. R., Bradley, D. D. C., Giles, M., Mcculloch, I., Ha, C.-S., & Ree, M. (2006). *Nat. Mater.*, *5*, 197.
[36] Chang, Y. M., & Wang, L. (2008). *J. Phys. Chem. C*, *112*, 17716.
[37] Ismail, Y. A. M., Soga, T., & Jimbo, T. (2009). *Sol. Energy Mater. Sol. Cells*, *93*, 1582.
[38] Erb, T., Zhokhavets, U., Gobsch, G., Raleva, S., Stuhn, B., Schilinsky, P., Waldauf, C., & Brabec, C. J. (2005). *Adv. Funct. Mater.*, *15*, 1193.
[39] Reyes-Reyes, M., López-Sandoval, R., Arenas-Alatorre, J., Garibay-Alonso, R., Carroll, D. L., & Lastras-Martinez, A. (2007). *Thin Solid Films*, *516*, 52.
[40] Briks, L. S., & Friedman, H. (1946). *J. Appl. Phys.*, *17*, 687.
[41] Liu, J., Shi, Y., & Yang, Y. (2001). *Adv. Funct. Mater.*, *11*, 420.
[42] Hope, H., Niggemann, M., Winder, C., Kraut, J., Hiesgen, R., Hinsch, A., Meissner, D., & Sariciftci, N. S. (2004). *Adv. Funct. Mater.*, *14*, 1005.
[43] Scharber, M. C., Műhlbacher, D., Koppe, M., Denk, P., Waldauf, C., Heeger, A. J., & Brabec, C. J. (2006). *Adv. Mater.*, *18*, 789.